Nonlinear Dyn (2020) 100:435–449
https://doi.org/10.1007/s11071-020-05531-8

ORIGINAL PAPER

Low-complexity hypersonic flight control with asymmetric angle of attack constraint

Hao An · Ziyi Guo · Guan Wang · Changhong Wang

Received: 19 October 2019 / Accepted: 11 February 2020 / Published online: 18 February 2020

Abstract This study investigates the longitudinal flight control problem of air-breathing hypersonic vehicles subject to the asymmetric angle of attack (AoA) constraint. With the help of introduced tangent errors, the proposed control becomes low complexity in both structure and expression, especially for the non-adaptive control algorithm in the altitude loop. The asymmetric AoA constraint, which is more practical in comparison with the previously considered symmetric AoA constraint, is well accommodated. Output tracking errors are regulated into small residual sets within the designated convergence time. Uncertain aerodynamic coefficients, structural flexibilities and scramjet input saturation are synthetically handled, making the proposed control competent for a real hypersonic flight mission.

Keywords Air-breathing hypersonic vehicle · Flight control · Low complexity · Asymmetric angle of attack constraint

List of symbols

$\bar{c}$	Mean aerodynamic chord
C_*^*	Polynomial fitting coefficients
D	Drag
g	Acceleration due to gravity
h	Altitude
I_{yy}	Moment of inertia
L	Lift
m	Mass
M_{yy}	Pitching moment
N_i	Generalized force for elastic mode η_i
$\bar{q}$	Dynamic pressure
Q	Pitch rate
S	Reference area
T	Thrust
V	Velocity
z_T	Thrust moment arm
α	Angle of attack
δ_{c}	Canard deflection angle
δ_{e}	Elevator deflection angle
η_i	ith generalized elastic coordinate
γ	Flight path angle
ω_i	Natural frequency for elastic mode η_i
Φ, Φ_{com}	Fuel-to-air equivalency ratio and its command
ψ_i, ψ_i'	Coupling coefficients
ξ_i	Damping ratio for elastic mode η_i

H. An (✉)· Z. Guo · G. Wang · C. Wang
Space Control and Inertial Technology Research Center, Harbin Institute of Technology, Harbin 150001, P. R. China
e-mail: hao.rc.an@gmail.com

1 Introduction

The research on air-breathing hypersonic vehicles (AHVs) has always been a worldwide hotspot in the last decades. As the biggest superiority over traditional aeronautic vehicles, AHVs are able to cruise or maneu-

ver at hypersonic speed with high efficiency, thanks to the advanced propulsion system of scramjet. In order to adapt the harsh flight environment, AHVs are usually configured as the waverider, whose dynamics include but are not limited to high nonlinearities, large uncertainties, strong couplings and unpredictable flexibilities, complicating the flight control system design [10].

Historically, numerous theoretical studies on the control of AHVs have sprung up [34]. Early research interests focus on the simplification of flight dynamics of AHVs using nonlinear dynamic inverse (NDI) or state feedback linearization (SFL). [30] combines the NDI and the linear quadratic regulator, which achieves the good tracking performance for AHVs cruising around 15 Mach. [37] combines the SFL and the sliding mode control, whose main advantage is the strong robustness with respect to modeling uncertainties. Recently, [3] combines the SFL and the observer-based anti-windup control to deal with external disturbances and actuator constraints. [26] combines the SFL and the neural dynamic surface control to handle both matched and unmatched uncertainties. [21] combines the SFL and the terminal sliding mode control to realize the output fast tracking. [7] proposes an adaptive higher-order sliding mode control for a linearized AHV model, which regulates the tracking error to a minimum in finite time.

Just as every coin has two sides, in order to realize NDI or SFL, designers must strategically neglect specific nonlinearities or couplings of AHVs, such as the structural flexibility aroused by the elongated fuselage, the nose-up pitching moment contributed by the hanging scramjet and the non-minimum phase property caused by the elevator-to-lift coupling, some of which have been proved crucial to a real hypersonic flight [17,23]. To overcome this deficiency, the well-known back-stepping design method [20] has been widely applied to the control of AHV models containing more flight characteristics. [36] introduces neural networks and disturbance observers in the back-stepping design for AHVs to obtain the strong robustness with respect to external disturbances and wind effects. [12,13] employ neural networks in the back-stepping design for AHVs to cope with nonaffine effects in the vehicle model. [14] uses fuzzy wavelet neural networks in the adaptive critic design for AHVs to guarantee the predefined tracking performance. In recent years, the fault-tolerant control has always been a research hotspot in both control theory [31–33] and hypersonic flight [2,25,28]. [25] applies the Takagi-Sugeno fuzzy control to overcome the actuator fault of AHVs. [2] enhances the traditional back-stepping design with the disturbance observer and the anti-windup mechanism to handle external disturbances, input constraints and faulty actuators of AHVs. [28] uses the terminal sliding mode technique to achieve both output fast tracking and actuator fault tolerance for AHVs.

To deal with unpredictable aerodynamic coefficients, [15,16] construct update laws for uncertain modeling parameters during the back-stepping design, resulting in the adaptive back-stepping control of AHVs. [1] further integrates the adaptive back-stepping design with the anti-windup mechanism, while giving a theoretical analysis on velocity and altitude tracking performances. [18] enhances the dynamic surface back-stepping design with the adaptive fault-tolerant mechanism, where time-varying uncertainties and actuator faults are overcome. [5] utilizes the multiple Lyapunov function technique in the adaptive back-stepping design for a switched control-oriented AHV model, which provides a possible solution to the full-envelope control problem of AHVs. Though modeling uncertainties, especially aerodynamic coefficients, have been successfully accommodated by the above-mentioned adaptive back-stepping designs [1,5,15,16,18], the corresponding control algorithms are somewhat complicated by nature because of the recursive design procedures, accompanied with extremely high dynamic orders caused by numerous parameter update laws [20]. To reduce the dynamic order of the adaptive control, [4] introduces a bound estimation mechanism to the command-filtered adaptive back-stepping design for AHVs, which requires less parameter update laws in comparison with [1,5,15,16,18]. Even so, the resulting control algorithm still involves relatively complicated expressions with four additional command filters. In view of the strict real-time requirement on the flight control system of AHVs, further researches on the complexity reduction for control algorithms become necessary and practical.

In hypersonic flight, angle of attack (AoA) is an important flight state affecting scramjet efficiency [23], which can be measured by the flush airdata sensing system [8]. Theoretical analysis in [11] indicates that the direction of the bow shock has close relationships to Mach number and AoA. Experimental result in [27] concludes that AoA needs to be limited within some feasible range to ensure the preferred scramjet work-

ing condition. At the same time, the improper AoA may cause extremely high heat flow at the belly or back of AHVs, in which case the coated thermal protection material becomes inefficient [17]. It is seen from the above observations that AoA should be strictly constrained during the entire hypersonic flight mission. Focusing on the AoA constrained hypersonic flight control problem, [24] makes the pioneering effort by developing a reference generation module to produce admissible references, but the flight dynamics under consideration is largely simplified. Later, [6] introduces barrier functions to the adaptive back-stepping design for AHVs to limit the magnitudes of flight states. [35] combines barrier functions with radial basis function neural networks in the back-stepping design for AHVs to limit AoA. However, the AoA constraints considered in [6,24,35] are symmetric, which may be relatively conservative and impractical for a real hypersonic flight mission. For example, the positive AoA is preferred in engineering to ensure the high-efficiency scramjet output, and the negative AoA probably induces the fatal scramjet flameout. Therefore, the asymmetric AoA constraint should be considered in the flight control system design, which has not been paid sufficient attentions in the literature.

Motivated by the previous observations, this study focuses on the low-complexity control problem of AHVs subject to the asymmetric AoA constraint, whose the main contribution lies in two aspects.

(1) The proposed control has the lower complexity in both structure and expression compared with the previous adaptive control works like [1,4,5,15,16,18], especially for the presented non-adaptive altitude-loop control.
(2) The proposed control handles the asymmetric AoA constraint, which is more practical compared with the previous AoA constrained control works like [6,24,35].

In addition, uncertain aerodynamic coefficients, structural flexibilities and fuel-to-air equivalency ratio (FER) saturation property are taken into account, synthetically. The convergence time of the output tracking error is designated without using complicated techniques like terminal or higher-order sliding mode control [7,21], leading to an easier realization of the control algorithm.

The rest of this study is organized as follows: Sect. 2 provides the necessary preliminaries including the considered AHV model, the introduced reference governor and the desired control objective. Section 3 presents the main results including the design and analysis processes for both velocity and altitude loops. Section 4 shows a simulation to verify the proposed control. Section 5 gives the conclusion.

2 Preliminaries

2.1 Vehicle model

The longitudinal motion of AHVs involves five rigid body flight states, namely velocity V, altitude h, flight path angle (FPA) γ, AoA α and pitch rate (PR) Q. Three control inputs are needed, namely, FER Φ, canard deflection angle (CDA) δ_{c} and elevator deflection angle (EDA) δ_{e}. More specifically, FER decides the combustion condition of scramjet and controls the thrust, while CDA and EDA collectively affect the longitudinal flight attitude of AHVs. To further consider the structural flexibilities, up to the second-order or third-order elastic modes are usually modeled. Similar to the handling in [29,36], the effect of structural flexibilities is equivalent to a time-varying bounded disturbance acting on the PR dynamics.

The vehicle model under consideration is borrowed from the longitudinal control-oriented model developed in [22], containing six dynamical and kinematic equations as

$$\dot{V} = \frac{T\cos\alpha - D}{m} - g\sin\gamma \tag{1}$$

$$\dot{h} = V\sin\gamma \tag{2}$$

$$\dot{\gamma} = \frac{T\sin\alpha + L}{mV} - \frac{g\cos\gamma}{V} \tag{3}$$

$$\dot{\alpha} = Q - \dot{\gamma} \tag{4}$$

$$\dot{Q} = \frac{M_{\mathrm{yy}}}{I_{\mathrm{yy}}} + \sum_{i=1}^{2}\frac{\psi_i\ddot{\eta}_i}{I_{\mathrm{yy}}} \tag{5}$$

$$\ddot{\eta}_i = -2\xi_i\omega_i\dot{\eta}_i - \omega_i^2\eta_i + N_i + \psi_i'\dot{Q}, \quad i = 1,2 \tag{6}$$

where the involved force and moment are formulated as

$$L = \bar{q}S\left(C_L^1\alpha + C_L^0 + C_L^{\delta_{\mathrm{c}}}\delta_{\mathrm{c}} + C_L^{\delta_{\mathrm{e}}}\delta_{\mathrm{e}}\right) \tag{7}$$

$$D = \bar{q}S\left(C_D^2\alpha^2 + C_D^1\alpha + C_D^0 + C_D^{\delta_{\mathrm{c}}^2}\delta_{\mathrm{c}}^2\right.$$

$$+ C_D^{\delta_c}\delta_c + C_D^{\delta_e^2}\delta_e^2 + C_D^{\delta_e}\delta_e\Big) \tag{8}$$

$$M_{yy} = z_T T + \bar{q}\bar{c}S\Big(C_M^2\alpha^2 + C_M^1\alpha + C_M^0 + C_M^{\delta_c}\delta_c + C_M^{\delta_e}\delta_e\Big) \tag{9}$$

$$T = \bar{q}S\Big[C_T^3\alpha^3 + C_T^2\alpha^2 + C_T^1\alpha + C_T^0 + \big(C_{T,\Phi}^3\alpha^3 + C_{T,\Phi}^2\alpha^2 + C_{T,\Phi}^1\alpha + C_{T,\Phi}^0\big)\Phi\Big] \tag{10}$$

$$N_1 = C_{N_1}^2\alpha^2 + C_{N_1}^1\alpha + C_{N_1}^0 \tag{11}$$

$$N_2 = C_{N_2}^2\alpha^2 + C_{N_2}^1\alpha + C_{N_2}^0 + C_{N_2}^{\delta_c}\delta_c + C_{N_2}^{\delta_e}\delta_e. \tag{12}$$

All the variable definitions in (1)–(12) are given in the nomenclature. More details on the employed vehicle model can be found in previous works like [11,22], which have been omitted here for page limitation. Considering that the current hypersonic technique is not mature enough to precisely calculate or predict the real aerodynamics of AHVs, a practical assumption is made on the vehicle model.

Assumption 1 The coefficients C_X^*, $X = L, D, M$ in the aerodynamic force and moment expressions (7)–(9) are uncertain, time-varying and bounded. The coefficients C_Y^*, $Y = T, N_1, N_2$ in the thrust and generalized force expressions (10)–(12) are uncertain constants.

2.2 Reference governors

2.2.1 Velocity reference governor

Before executing a hypersonic flight mission, the nominal trajectory should be planned first. Traditional velocity reference is usually generated by a simple command filter, whose main purpose is to smooth the step velocity command given by the onboard pilot or the ground control. However, such trajectory planning can hardly take into account the practical FER saturation property, having a general form as

$$\Phi = \mathrm{Sat}(\Phi_{\mathrm{com}}) = \begin{cases} \Phi_{\mathrm{cooling}}, & \Phi_{\mathrm{com}} < \Phi_{\mathrm{cooling}} \\ \Phi_{\mathrm{choking}}, & \Phi_{\mathrm{com}} > \Phi_{\mathrm{choking}} \\ \Phi_{\mathrm{com}}, & \text{otherwise} \end{cases} \tag{13}$$

where Φ_{com} is the control command of FER; Φ_{choking} is the upper threshold of FER in case of the scramjet thermal choking; Φ_{cooling} is the lower threshold of FER set for the scramjet active cooling.

Remark 1 Thermal choking is an important factor that affects the scramjet operation and must be avoided during hypersonic flight. Theoretical and experimental results show that the relatively large FER makes the airflow speed at the combustor exit become around 1 Mach, causing the scramjet to choke [38]. In engineering, the aggressive velocity reference may induce the real FER to be larger than its upper threshold, in which case the scramjet thermal choking happens.

To accommodate the above FER saturation, inspired by [1], an adaptive reference governor is employed to adjust the velocity reference according to the FER saturation level, formulated as

$$\begin{cases} V_{\mathrm{ref}} = V_{\mathrm{des}} + V_{\mathrm{adj}} \\ \dot{V}_{\mathrm{adj}} = \hat{\boldsymbol{\Theta}}_\Phi^{\mathrm{T}}\boldsymbol{\Psi}_\Phi\Big[\mathrm{Sat}(\Phi_{\mathrm{com}}) - \Phi_{\mathrm{com}}\Big] - k_V V_{\mathrm{adj}} \end{cases} \tag{14}$$

where V_{ref} denotes the real velocity reference; V_{des} denotes the desired velocity reference generated by the traditional second-order command filter [16]; V_{adj} is the adjusting signal related to the FER saturation level, and $V_{\mathrm{adj}}(0) = 0$; $\boldsymbol{\Psi}_\Phi \in \mathbb{R}^4$ is defined as (24); $\hat{\boldsymbol{\Theta}}_\Phi \in \mathbb{R}^4$ is obtained from the parameter update law (31); $k_V > 0$.

2.2.2 FPA reference governor

For the nonlinear kinematical equation (2), the small-angle approximation $\sin\gamma \approx \gamma$ is usually applied [1,16]. However, for the longitudinal maneuver of AHVs, the real FPA may become undesirably large (for example, $\gamma > 3$ deg), invalidating the above small-angle approximation. To remedy this deficiency as well as to simplify the altitude-loop back-stepping design, inspired by [15], an FPA reference governor is introduced as

$$\gamma_{\mathrm{ref}} = \arcsin\left[\frac{-k_h\big(h - h_{\mathrm{ref}}\big) + \dot{h}_{\mathrm{ref}}}{V}\right] \tag{15}$$

where h_{ref} is the smooth altitude reference generated by the traditional second-order command filter; $k_h > 0$.

2.3 Control objective

For the considered vehicle model (1)–(12) and the predesigned reference governors (14) and (15), the control objective of this study is to ensure the bounded stability of the closed-loop AHV system in spite of uncertain aerodynamic coefficients, structural flexibilities and FER saturation property, along with three additional features.

- *Feature 1 low-complexity control algorithm.* In order to save the valuable computing resource of the airborne computer, the proposed control needs to be as simple as possible in both structure and expression.
- *Feature 2 asymmetric AoA constraint.* In order to ensure the high-efficiency scramjet working, AoA should be kept around a nominal AoA function, which is equivalent to the asymmetric AoA constraint.
- *Feature 3 designated convergence time.* In order to achieve the fast and precise tracking, output tracking errors are preferred to be regulated into small residual sets before the designated convergence time.

3 Main results

According to the structure of the vehicle model, the longitudinal control of AHVs is decomposed into velocity loop and altitude loop (or the equivalent FPA loop in this study). This section will present design procedures for both velocity and altitude loops, respectively.

3.1 Velocity reference tracking with FER saturation and designated convergence time

In engineering, the initial velocity tracking error is introduced by multiple factors like the imprecise velocity measurement, whose value is supposed to be inside a feasible initial set $\mathbb{E}_{V,0} = \{e_{V,0} : |e_{V,0}| < \varpi_{V,0}\}$ with $\varpi_{V,0}$ denoting a properly large constant. One control objective of this study is to regulate the velocity tracking error $e_V = V - V_{\text{ref}}$ satisfying $e_V(0) \in \mathbb{E}_{V,0}$ to the residual set $\mathbb{E}_{V,\text{des}} = \{e_{V,\text{des}} : |e_{V,\text{des}}| < \varpi_{V,\text{des}}\}$ with the maximal convergence time $t_{V,\text{con}}$, where $\varpi_{V,\text{des}}$ is a small positive constant selected according to the final tracking precision.

Remark 2 Note that the velocity is a key flight state since it decides the dynamic pressure $\bar{q} = 0.5\rho V^2$, where ρ is the air density. Any fluctuation in velocity may cause obvious variations in scramjet thrust and aerodynamic force and moment, see (7)–(10), which further disturb the flight dynamics. What is more, the thermal protection system of AHVs usually works near its design limit for the extremely high aerodynamic heat at hypersonic speed. Therefore, the velocity of AHVs should be carefully planned and regulated to avoid the overheating of the thermal protection system. Based on the above considerations, it is necessary to designate a performance index for the velocity tracking error.

Without loss of generality, this study assumes the initial time instant $t_0 = 0$. To realize the velocity tracking performance, a positive bound function is defined as

$$\beta_V(t) = \left(\varpi_{V,0} - \varpi_{V,\infty}\right)\mathrm{e}^{-\tau_V t} + \varpi_{V,\infty} \tag{16}$$

where $0 < \varpi_{V,\infty} < \varpi_{V,\text{des}} < \varpi_{V,0}$. If $|e_V(t)| < \beta_V(t)$ is satisfied, the maximal convergence time of velocity tracking error e_V from initial set $\mathbb{E}_{V,0}$ to residual set $\mathbb{E}_{V,\text{des}}$ is $\frac{1}{\tau_V}\ln\left(\frac{\varpi_{V,0} - \varpi_{V,\infty}}{\varpi_{V,\text{des}} - \varpi_{V,\infty}}\right)$. In other words, to guarantee the designated convergence time $t_{V,\text{con}}$, the parameter τ_V in function $\beta_V(t)$ should be selected satisfying

$$\tau_V > \frac{1}{t_{V,\text{con}}}\ln\left(\frac{\varpi_{V,0} - \varpi_{V,\infty}}{\varpi_{V,\text{des}} - \varpi_{V,\infty}}\right). \tag{17}$$

Remark 3 For the designated tracking precision $\varpi_{V,\text{des}}$ and convergence time $t_{V,\text{con}}$, the parameter selection for the performance function $\beta_V(t)$ refers to the following rules: $\varpi_{V,\infty}$ is properly smaller than $\varpi_{V,\text{des}}$; $\varpi_{V,0}$ is conservatively large according to the experimental information of the velocity measuring error; τ_V is selected satisfying (17).

To further realize $|e_V(t)| < \beta_V(t)$, a new tangent error is introduced as

$$e_{V,\tan} = \tan\left(\frac{\pi e_V}{2\beta_V}\right) \tag{18}$$

whose time derivative is calculated as

$$\dot{e}_{V,\tan} = \frac{\pi(1 + e_{V,\tan}^2)}{2\beta_V}\left(\dot{e}_V - \frac{\dot{\beta}_V}{\beta_V}e_V\right). \tag{19}$$

Obviously, $e_V = 0$ corresponds to $e_{V,\tan} = 0$. And also, if $e_V \to \beta_V^-$ (or $e_V \to -\beta_V^+$), $e_{V,\tan} \to +\infty$ (or $e_{V,\tan} \to -\infty$). Under the precondition of $e_V(0) \in \mathbb{E}_{V,0}$ (i.e., $|e_V(0)| < \beta_V(0)$), the desired $|e_V(t)| < \beta_V(t)$ can be achieved as long as the proposed control guarantees the boundedness of the introduced tangent error $e_{V,\tan}$. Such tangent error is somewhat inspired by [9], where a logarithmic auxiliary function is employed to realize a low-complexity control scheme for pure feedback systems.

Using the dynamical equation (1), the time derivative of the velocity tracking error can be rewritten into a parameterized form as

$$\begin{aligned}\dot{e}_V = &-g\sin\gamma - \dot{V}_{\text{des}} + k_V V_{\text{adj}} + \boldsymbol{\Theta}_V^{\mathrm{T}}\boldsymbol{\Psi}_V \\ &+ \hat{\boldsymbol{\Theta}}_\Phi^{\mathrm{T}}\boldsymbol{\Psi}_\Phi\Phi_{\text{com}} + \tilde{\boldsymbol{\Theta}}_\Phi^{\mathrm{T}}\boldsymbol{\Psi}_\Phi \text{Sat}(\Phi_{\text{com}})\end{aligned} \tag{20}$$

where $\hat{\bullet}$ denotes an estimate of the uncertain parameter or vector $\bullet$, $\tilde{\bullet} = \bullet - \hat{\bullet}$; $\boldsymbol{\Theta}_V$, $\boldsymbol{\Psi}_V$, $\boldsymbol{\Theta}_\Phi$ and $\boldsymbol{\Psi}_\Phi$ are defined as

$$\begin{aligned}\boldsymbol{\Theta}_V = &\Big[C_T^3,\ C_T^2,\ C_T^1,\ C_T^0,\ C_D^2,\ C_D^1, \\ &C_D^0,\ C_D^{\delta_c^2},\ C_D^{\delta_c},\ C_D^{\delta_e^2},\ C_D^{\delta_e}\Big]^{\mathrm{T}}\end{aligned} \tag{21}$$

$$\begin{aligned}\boldsymbol{\Psi}_V = &\frac{\bar{q}S}{m}\Big[\alpha^3\cos\alpha,\ \alpha^2\cos\alpha,\ \alpha\cos\alpha,\ \cos\alpha,\ -\alpha^2, \\ &-\alpha,\ -1,\ -\delta_c^2,\ -\delta_c,\ -\delta_e^2,\ -\delta_e\Big]^{\mathrm{T}}\end{aligned} \tag{22}$$

$$\boldsymbol{\Theta}_\Phi = \Big[C_{T,\Phi}^3,\ C_{T,\Phi}^2,\ C_{T,\Phi}^1,\ C_{T,\Phi}^0\Big]^{\mathrm{T}} \tag{23}$$

$$\boldsymbol{\Psi}_\Phi = \frac{\bar{q}S\cos\alpha}{m}\Big[\alpha^3,\ \alpha^2,\ \alpha,\ 1\Big]^{\mathrm{T}}. \tag{24}$$

Consider a quadratic function:

$$\mathcal{Q}_V = \frac{e_{V,\tan}^2}{2} \tag{25}$$

whose time derivative, using (19) and (20), is calculated as

$$\begin{aligned}\dot{\mathcal{Q}}_V = &\Upsilon_V(e_{V,\tan},t)e_{V,\tan}\Big(-\frac{\dot{\beta}_V e_V}{\beta_V} - g\sin\gamma - \dot{V}_{\text{des}} \\ &+ k_V V_{\text{adj}} + \boldsymbol{\Theta}_V^{\mathrm{T}}\boldsymbol{\Psi}_V + \hat{\boldsymbol{\Theta}}_\Phi^{\mathrm{T}}\boldsymbol{\Psi}_\Phi\Phi_{\text{com}}\Big) \\ &+ \Upsilon_V(e_{V,\tan},t)e_{V,\tan}\tilde{\boldsymbol{\Theta}}_\Phi^{\mathrm{T}}\boldsymbol{\Psi}_\Phi\text{Sat}(\Phi_{\text{com}})\end{aligned} \tag{26}$$

with $\Upsilon_V(e_{V,\tan},t) = \dfrac{\pi(1+e_{V,\tan}^2)}{2\beta_V} \geq \dfrac{\pi}{2\beta_V}$.

Remark 4 Aiming at the uncertain parameter vector $\boldsymbol{\Theta}_V \in \mathbb{R}^{11}$, the traditional adaptive estimation method in [15,16] that constructs a parameter update law for $\boldsymbol{\Theta}_V$ can be utilized. However, $\boldsymbol{\Theta}_V$ has to be assumed constant or slow time-varying, while the dynamic order of the corresponding parameter update law will become as high as eleven.

For the purpose of handling the uncertain time-varying $\boldsymbol{\Theta}_V$ as well as reducing the dynamic order, inspired by [4], a norm bound of $\boldsymbol{\Theta}_V$ is introduced as $\Theta = \sup\{||\boldsymbol{\Theta}_V(t)||\}$. As a result, the uncertain term $\Upsilon_V(e_{V,\tan},t)e_{V,\tan}\boldsymbol{\Theta}_V^{\mathrm{T}}\boldsymbol{\Psi}_V$ in (26) satisfies

$$\begin{aligned}\Upsilon_V e_{V,\tan}\boldsymbol{\Theta}_V^{\mathrm{T}}\boldsymbol{\Psi}_V \leq\ &\Upsilon_V|e_{V,\tan}|||\boldsymbol{\Psi}_V||\tilde{\Theta} + \varepsilon \\ &+ \Upsilon_V e_{V,\tan}||\boldsymbol{\Psi}_V||\hat{\Theta}\tanh\Big(\frac{c\Upsilon_V e_{V,\tan}||\boldsymbol{\Psi}_V||\hat{\Theta}}{\varepsilon}\Big)\end{aligned} \tag{27}$$

where $c \approx 0.2785$ and $\varepsilon > 0$; the inequality $|\bullet| \leq \bullet\tanh\left(\frac{c\bullet}{\varepsilon}\right) + \varepsilon$ has been applied; the elements $e_{V,\tan}$ and t in function $\Upsilon_V(e_{V,\tan},t)$ have been neglected for clarity. Substituting (27) into (26), it has

$$\begin{aligned}\dot{\mathcal{Q}}_V \leq\ &\Upsilon_V e_{V,\tan}\Big[-\frac{\dot{\beta}_V e_V}{\beta_V} - g\sin\gamma - \dot{V}_{\text{des}} + k_V V_{\text{adj}} \\ &+ ||\boldsymbol{\Psi}_V||\hat{\Theta}\tanh\Big(\frac{c\Upsilon_V e_{V,\tan}||\boldsymbol{\Psi}_V||\hat{\Theta}}{\varepsilon}\Big) \\ &+ \hat{\boldsymbol{\Theta}}_\Phi^{\mathrm{T}}\boldsymbol{\Psi}_\Phi\Phi_{\text{com}}\Big] + \Upsilon_V e_{V,\tan}\tilde{\boldsymbol{\Theta}}_\Phi^{\mathrm{T}}\boldsymbol{\Psi}_\Phi\text{Sat}(\Phi_{\text{com}}) \\ &+ \Upsilon_V|e_{V,\tan}|||\boldsymbol{\Psi}_V||\tilde{\Theta} + \varepsilon.\end{aligned} \tag{28}$$

In view of (28), the adaptive FER control algorithm is designed as

$$\begin{aligned}\Phi_{\text{com}} = &\frac{1}{\hat{\boldsymbol{\Theta}}_\Phi^{\mathrm{T}}\boldsymbol{\Psi}_\Phi}\Big[-\frac{k_V e_{V,\tan}}{\Upsilon_V} + \frac{\dot{\beta}_V e_V}{\beta_V} \\ &+ g\sin\gamma + \dot{V}_{\text{des}} - k_V V_{\text{adj}} \\ &- ||\boldsymbol{\Psi}_V||\hat{\Theta}\tanh\Big(\frac{c\Upsilon_V e_{V,\tan}||\boldsymbol{\Psi}_V||\hat{\Theta}}{\varepsilon}\Big)\Big]\end{aligned} \tag{29}$$

with the parameter update laws of $\hat{\Theta}$ and $\hat{\boldsymbol{\Theta}}_\Phi$ constructed as

$$\dot{\hat{\Theta}} = \frac{1}{\varrho_{V,1}}\left(\Upsilon_V |e_{V,\tan}| ||\boldsymbol{\Psi}_V|| - \kappa_{V,1}\hat{\Theta}\right) \tag{30}$$

$$\dot{\hat{\boldsymbol{\Theta}}}_\Phi = \mathrm{Proj}\left\{\frac{1}{\varrho_{V,2}}\left[\Upsilon_V e_{V,\tan}\boldsymbol{\Psi}_\Phi \mathrm{Sat}(\Phi_{\mathrm{com}}) - \kappa_{V,2}\hat{\boldsymbol{\Theta}}_\Phi\right]\right\} \tag{31}$$

where $\varrho_{V,i} > 0$, $\kappa_{V,i} > 0$, $i = 1, 2$; Proj$\{\bullet\}$ is the parameter projection ensuring the updated $\hat{\boldsymbol{\Theta}}_\Phi$ always within the allowable set [20] and has been widely applied in the control of AHVs [1,16].

Up to now, the design process for the velocity loop has been finished. To further analyze the effectiveness of the proposed control, a quadratic Lyapunov function is constructed as

$$\mathcal{L}_V = \mathcal{Q}_V + \frac{\varrho_{V,1}\tilde{\Theta}^2}{2} + \frac{\varrho_{V,2}||\tilde{\boldsymbol{\Theta}}_\Phi||^2}{2} \tag{32}$$

whose time derivative, combining (28)–(31) and applying the inequality $2\tilde{\bullet}\hat{\bullet} \le ||\bullet||^2 - ||\tilde{\bullet}||^2$, satisfies

$$\dot{\mathcal{L}}_V \le -a_V\mathcal{L}_V + b_V \tag{33}$$

with $a_V = \min\left\{2k_V, \frac{\kappa_{V,1}}{\varrho_{V,1}}, \frac{\kappa_{V,2}}{\varrho_{V,2}}\right\}$, $b_V = \varepsilon + \frac{\kappa_{V,1}\Theta^2}{2} + \frac{\kappa_{V,2}||\boldsymbol{\Theta}_\Phi||^2}{2}$. Obviously, $\dot{\mathcal{L}}_V < 0$ provided that $\mathcal{L}_V > \frac{b_V}{a_V}$. As a result, the introduced tangent error $e_{V,\tan}$ is bounded as $|e_{V,\tan}| \le \lambda_V = \sqrt{2\max\left\{\mathcal{L}_V(0), \frac{b_V}{a_V}\right\}}$, implying that the designated tracking precision $\varpi_{V,\mathrm{des}}$ and convergence time $t_{V,\mathrm{con}}$ are achieved.

Remark 5 The proposed control algorithm for the velocity loop contains the velocity reference governor (14), the FER control law (29) and the parameter update laws (30), (31), whose dynamic order is much smaller than those of previous adaptive control works like [1,5,15,16]. It is seen from (33) and the above analysis that the tracking performance can be further improved by producing small b_V and large a_V. More specifically, properly small ε, $\kappa_{V,1}$, $\kappa_{V,2}$ are preferred to ensure small b_V, while properly large k_V and small $\varrho_{V,1}$, $\varrho_{V,2}$ (much smaller than $\kappa_{V,1}$, $\kappa_{V,2}$, respectively) are preferred to ensure large a_V.

3.2 FPA reference tracking with asymmetric AoA constraint and designated convergence time

Before design, define error variables:

$$e_\gamma = \gamma - \gamma_{\mathrm{ref}},\ e_x = x - v_x \tag{34}$$

for $x = \alpha, Q$, where v_α and v_Q are virtual controls introduced for the back-stepping design. To improve the tracking performance, the FPA tracking error should be limited as $|e_\gamma(t)| < \beta_\gamma(t)$, where the bound function $\beta_\gamma(t)$ is designed similar to $\beta_V(t)$ in the velocity loop, ensuring the designated tracking precision and convergence time. In addition, it will be shown later that the design of $\beta_\gamma(t)$ needs to consider the asymmetric AoA constraint at the same time.

Just as mentioned before, AoA needs to be strictly constrained within the asymmetric feasible set $\mathbb{S}_\alpha = \left\{\alpha(t) : \underline{\alpha}(t) < \alpha(t) < \overline{\alpha}(t)\right\}$. To guarantee this AoA constraint, the virtual control v_α is designed as

$$v_\alpha = \alpha_{\mathrm{nom}}(t) - e_\gamma \tag{35}$$

where $\alpha_{\mathrm{nom}}(t)$ is the preset nominal AoA function, and obviously, $\alpha_{\mathrm{nom}}(t) \in \mathbb{S}_\alpha$. In engineering, the nominal AoA function is selected according to the planned flight trajectory with synthetical considerations on multiple factors like the high-efficiency working condition for scramjet and the safe thermal flux for thermal protection system. Using (35), AoA can be rewritten as

$$\alpha = \alpha_{\mathrm{nom}}(t) - e_\gamma + e_\alpha. \tag{36}$$

If the error variables e_γ and e_α are constrained as

$$|e_\gamma(t)| < \beta_\gamma(t), \quad |e_\alpha(t)| < \beta_\alpha(t) \tag{37}$$

where $\beta_\gamma(t)$ and $\beta_\alpha(t)$ are positive functions properly designed to satisfy the relationship $\beta_\gamma(t) + \beta_\alpha(t) \le \min\left\{\overline{\alpha}(t) - \alpha_{\mathrm{nom}}(t),\ \alpha_{\mathrm{nom}}(t) - \underline{\alpha}(t)\right\}$, the prescribed AoA constraint $\alpha \in \mathbb{S}_\alpha$ is guaranteed.

To facilitate the design and analysis process, introduce three normalized errors:

$$e_{x,\mathrm{nor}} = \frac{e_x}{\beta_x} \tag{38}$$

and three tangent errors:

$$e_{x,\tan} = \tan\left(\frac{\pi e_{x,\mathrm{nor}}}{2}\right) \tag{39}$$

where $x = \gamma, \alpha, Q$; $\beta_Q(t)$ is the bound function of the error variable e_Q, that is, $|e_Q(t)| < \beta_Q(t)$. In what follows, the truncated solution of $(e_{\gamma,\mathrm{nor}}, e_{\alpha,\mathrm{nor}}, e_{Q,\mathrm{nor}}, t) \in \mathbb{I}^3 \times \mathbb{T}$ will be considered first, where $\mathbb{I} = (-1, 1)$; $\mathbb{T}$ denotes the maximal time interval with respect to $(e_{\gamma,\mathrm{nor}}, e_{\alpha,\mathrm{nor}}, e_{Q,\mathrm{nor}}) \in \mathbb{I}^3$. Then, it will be shown that the proposed control leads to the infinite property of $\mathbb{T}$, and thus, the prescribed limitation (37) can always be guaranteed during the entire flight mission.

3.2.1 CDA control algorithm

Using the dynamical equation (3), the time derivative of the normalized error $e_{\gamma,\mathrm{nor}}$ is formulated as

$$\dot{e}_{\gamma,\mathrm{nor}} = \frac{1}{\beta_\gamma}\left(\dot{e}_\gamma - \dot{\beta}_\gamma e_{\gamma,\mathrm{nor}}\right) = f_\gamma + g_\gamma \delta_\mathrm{c} \tag{40}$$

where $f_\gamma = \frac{1}{\beta_\gamma m V}\Big[T\sin\alpha + \bar{q}S\big(C_L^1\alpha + C_L^0 + C_L^{\delta_\mathrm{e}}\delta_\mathrm{e}\big) - mg\cos\gamma - mV\big(\dot{\gamma}_\mathrm{ref} + \dot{\beta}_\gamma e_{\gamma,\mathrm{nor}}\big)\Big]$, $g_\gamma = \frac{\bar{q}SC_L^{\delta_\mathrm{c}}}{\beta_\gamma m V}$. Consider that

- *Fact 1* $T\sin\alpha$ is the thrust component along the direction of lift, whose effect is weak because of the small AoA and is usually neglected or regarded as a bounded disturbance;
- *Fact 2* $\bar{q}S\big(C_L^1\alpha + C_L^0\big)$ and $\bar{q}SC_L^{\delta_\mathrm{e}}\delta_\mathrm{e}$ are the lift components contributed by body and elevator, respectively, which are bounded in reality;
- *Fact 3* $\dot{\gamma}_\mathrm{ref}$ is predesigned to be bounded, and $\dot{\beta}_\gamma e_{\gamma,\mathrm{nor}}$ is bounded for the predesigned β_γ and the considered $e_{\gamma,\mathrm{nor}} \in \mathbb{I}$.

It is concluded from *Facts 1–3* that during $t \in \mathbb{T}$, $|f_\gamma|$ has a maximum denoted as $|f_\gamma|_{\max}$. Similarly, $|g_\gamma|$ has a nonzero minimum denoted as $|g_\gamma|_{\min}$. With the help of the introduced tangent error $e_{\gamma,\tan}$, a low-complexity CDA control algorithm is proposed as

$$\delta_\mathrm{c} = -\mathrm{sign}(g_\gamma)k_\gamma e_{\gamma,\tan} \tag{41}$$

where $k_\gamma > 0$. For analysis purpose, consider the quadratic function:

$$\mathcal{Q}_\gamma = \frac{e_{\gamma,\tan}^2}{2} \tag{42}$$

whose time derivative, using (40) and (41), is calculated as

$$\dot{\mathcal{Q}}_\gamma \le \frac{\pi|e_{\gamma,\tan}|}{2\cos^2\left(\frac{\pi e_{\gamma,\mathrm{nor}}}{2}\right)}\Big(|f_\gamma| - k_\gamma|g_\gamma||e_{\gamma,\tan}|\Big). \tag{43}$$

Note that $\dot{\mathcal{Q}}_\gamma$ is well defined with respect to $e_{\gamma,\tan} \in \mathbb{I}$. It is seen from (43) that $\dot{\mathcal{Q}}_\gamma < 0$ if $|e_{\gamma,\tan}| > \frac{|f_\gamma|_{\max}}{k_\gamma|g_\gamma|_{\min}}$. As a result, the tangent error $e_{\gamma,\tan}$ is bounded as

$$|e_{\gamma,\tan}| \le \lambda_\gamma = \max\left\{|e_{\gamma,\tan}(0)|, \frac{|f_\gamma|_{\max}}{k_\gamma|g_\gamma|_{\min}}\right\} \tag{44}$$

and consequently, the normalized error $e_{\gamma,\mathrm{nor}}$ is bounded as

$$|e_{\gamma,\mathrm{nor}}| = \frac{|e_\gamma|}{\beta_\gamma} \le \frac{2\arctan(\lambda_\gamma)}{\pi} < 1. \tag{45}$$

Therefore, the constraint $|e_\gamma(t)| < \beta_\gamma(t)$ is guaranteed during $t \in \mathbb{T}$.

Remark 6 It should be reemphasized that the motivation of designating performance for the FPA tracking error comes from two aspects. On the one side, the prescribed FPA tracking performance improves the altitude tracking precision. More importantly, the constrained FPA tracking error is required in our design to accommodate the asymmetric AoA constraint.

3.2.2 EDA control algorithm

Combining the kinematic equation (4) and the virtual control (35), the time derivative of the error e_α is formulated as

$$\dot{e}_\alpha = e_Q + v_Q - \dot{\gamma}_\mathrm{ref} - \dot{\alpha}_\mathrm{nom}. \tag{46}$$

Using (46), the time derivative of the normalized error $e_{\alpha,\mathrm{nor}}$ becomes

$$\dot{e}_{\alpha,\mathrm{nor}} = \frac{1}{\beta_\alpha}\left(\dot{e}_\alpha - \dot{\beta}_\alpha e_{\alpha,\mathrm{nor}}\right) = f_\alpha + g_\alpha v_Q \tag{47}$$

where $f_\alpha = \frac{1}{\beta_\alpha}\left(\beta_Q e_{Q,\mathrm{nor}} - \dot{\gamma}_{\mathrm{ref}} - \dot{\alpha}_{\mathrm{nom}} - \dot{\beta}_\alpha e_{\alpha,\mathrm{nor}}\right)$, $g_\alpha = \frac{1}{\beta_\alpha}$. Regarding $(e_{\alpha,\mathrm{nor}},\ e_{Q,\mathrm{nor}},\ t) \in \mathbb{I}^2 \times \mathbb{T}$ and the predesigned β_α, β_Q, γ_{ref} and α_{nom}, $|f_\alpha|$ has a maximum denoted as $|f_\alpha|_{\max}$; meanwhile, $|g_\alpha|$ has a nonzero minimum, denoted as $|g_\alpha|_{\min}$. Then, a low-complexity virtual control algorithm is designed as

$$v_Q = -k_\alpha e_{\alpha,\tan} \tag{48}$$

where $k_\alpha > 0$. The time derivative of the virtual control v_Q is formulated as

$$\dot{v}_Q = -\frac{k_\alpha \pi \dot{e}_{\alpha,\mathrm{nor}}}{2\cos^2\left(\frac{\pi e_{\alpha,\mathrm{nor}}}{2}\right)} \tag{49}$$

where $\dot{v}_Q$ is well defined with respect to $e_{\alpha,\mathrm{nor}} \in \mathbb{I}$. Considering the quadratic function:

$$\mathcal{Q}_\alpha = \frac{e_{\alpha,\tan}^2}{2} \tag{50}$$

it is derived from (47) and (48) that

$$\dot{\mathcal{Q}}_\alpha \le \frac{\pi |e_{\alpha,\tan}|}{2\cos^2\left(\frac{\pi e_{\alpha,\mathrm{nor}}}{2}\right)}\left(|f_\alpha| - k_\alpha |g_\alpha||e_{\alpha,\tan}|\right). \tag{51}$$

Similarly, $\dot{\mathcal{Q}}_\alpha < 0$ if $|e_{\alpha,\tan}| > \frac{|f_\alpha|_{\max}}{k_\alpha |g_\alpha|_{\min}}$. This also derives that the tangent error $e_{\alpha,\tan}$ is bounded as

$$|e_{\alpha,\tan}| \le \lambda_\alpha = \max\left\{|e_{\alpha,\tan}(0)|,\ \frac{|f_\alpha|_{\max}}{k_\alpha |g_\alpha|_{\min}}\right\} \tag{52}$$

and moreover,

$$|e_{\alpha,\mathrm{nor}}| = \frac{|e_\alpha|}{\beta_\alpha} \le \frac{2\arctan(\lambda_\alpha)}{\pi} < 1 \tag{53}$$

$$\frac{1}{\cos^2\left(\frac{\pi e_{\alpha,\mathrm{nor}}}{2}\right)} = 1 + \tan^2\left(\frac{\pi e_{\alpha,\mathrm{nor}}}{2}\right) \le 1 + \lambda_\alpha^2. \tag{54}$$

Therefore, the constraint $|e_\alpha(t)| < \beta_\alpha(t)$ is guaranteed during $t \in \mathbb{T}$. Recalling (54) and the boundedness of $\dot{e}_{\alpha,\mathrm{nor}}$, the boundedness of $\dot{v}_Q$ calculated as (49) is also guaranteed.

Next, the PR dynamics is taken into account. Using the dynamical equation (6), the time derivative of the normalized error $e_{Q,\mathrm{nor}}$ is formulated as

$$\dot{e}_{Q,\mathrm{nor}} = \frac{1}{\beta_Q}\left(\dot{e}_Q - \dot{\beta}_Q e_{Q,\mathrm{nor}}\right) = f_Q + g_Q \delta_{\mathrm{e}} \tag{55}$$

where $f_Q = \frac{1}{\beta_Q I_{\mathrm{yy}}}\Big[z_T T + \bar{c}\bar{q}S\left(C_M^2\alpha^2 + C_M^1\alpha + C_M^0 + C_M^{\delta_{\mathrm{c}}}\delta_{\mathrm{c}}\right) + \sum_{i=1}^2 \psi_i \ddot{\eta}_i - I_{\mathrm{yy}}\left(\dot{v}_Q + \dot{\beta}_Q e_{Q,\mathrm{nor}}\right)\Big]$, $g_Q = \frac{\bar{c}\bar{q}SC_M^{\delta_{\mathrm{e}}}}{\beta_Q I_{\mathrm{yy}}}$. Consider that

- *Fact 4* $z_T T$, $\bar{c}\bar{q}S\left(C_M^2\alpha^2 + C_M^1\alpha + C_M^0\right)$ and $\bar{c}\bar{q}SC_M^{\delta_{\mathrm{c}}}\delta_{\mathrm{c}}$ are the pitching moments contributed by scramjet, body and canard, respectively, which are bounded in reality;
- *Fact 5* $\sum_{i=1}^2 \psi_i \ddot{\eta}_i$ is the effect of structural flexibilities on the PR dynamics, which is also bounded;
- *Fact 6* $\dot{v}_Q$ has been proved to be bounded hereinbefore, and $\dot{\beta}_Q e_{Q,\mathrm{nor}}$ is bounded for the predesigned β_Q and the considered $e_{Q,\mathrm{nor}} \in \mathbb{I}$.

It is concluded from *Facts 4–6* that during $t \in \mathbb{T}$, $|f_Q|$ has a maximum denoted as $|f_Q|_{\max}$. And similarly, $|g_Q|$ has a nonzero minimum denoted as $|g_Q|_{\min}$. A low-complexity EDA control algorithm is designed as

$$\delta_{\mathrm{e}} = -\mathrm{sign}(g_Q) k_Q e_{Q,\tan} \tag{56}$$

where $k_Q > 0$. Consider the quadratic function:

$$\mathcal{Q}_Q = \frac{e_{Q,\tan}^2}{2} \tag{57}$$

whose time derivative, combining (55) and (56), satisfies

$$\dot{\mathcal{Q}}_Q \le \frac{\pi |e_{Q,\tan}|}{2\cos^2\left(\frac{\pi e_{Q,\mathrm{nor}}}{2}\right)}\left(|f_Q| - k_Q |g_Q||e_{Q,\tan}|\right). \tag{58}$$

Furthermore, $\dot{\mathcal{Q}}_Q < 0$ if $|e_{Q,\tan}| > \frac{|f_Q|_{\max}}{k_Q |g_Q|_{\min}}$. This also indicates that the tangent error $e_{Q,\tan}$ and the normalized error $e_{Q,\mathrm{nor}}$ are bounded as

$$|e_{Q,\tan}| \le \lambda_Q = \max\left\{|e_{Q,\tan}(0)|,\ \frac{|f_Q|_{\max}}{k_Q |g_Q|_{\min}}\right\} \tag{59}$$

$$|e_{Q,\mathrm{nor}}| = \frac{|e_Q|}{\beta_Q} \leq \frac{2\arctan(\lambda_Q)}{\pi} < 1. \tag{60}$$

Therefore, the constraint $|e_Q(t)| < \beta_Q(t)$ is guaranteed during $t \in \mathbb{T}$.

Remark 7 The proposed control algorithm for the altitude loop contains the FPA reference governor (15), the virtual control laws (35), (48), the CDA control law (41) and the EDA control law (56), which involves no parameter update law and has the lower complexity in both structure and expression compared with previous adaptive control works like [1,5,15,16,18].

3.2.3 Extension of time interval $\mathbb{T}$

So far, the control design and performance analysis have been given for the maximal time interval $\mathbb{T}$, during which $(e_{\gamma,\mathrm{nor}},\ e_{\alpha,\mathrm{nor}},\ e_{Q,\mathrm{nor}}) \in \mathbb{I}^3$. However, if $\mathbb{T}$ does not cover the desired flight mission, for example $t_{\mathrm{con}} \notin \mathbb{T}$, the control objective cannot be achieved anymore. What is more, it is difficult to calculate or estimate $\mathbb{T}$, making the further analysis on its property become necessary. In fact, $\mathbb{T}$ can be extended to $[0, +\infty)$ under the proposed control, provided that the initial condition $(e_{\gamma,\mathrm{nor}}(0),\ e_{\alpha,\mathrm{nor}}(0),\ e_{Q,\mathrm{nor}}(0)) \in \mathbb{I}^3$ is satisfied. The following analysis is inspired from the proof philosophy of Theorem 3.3 in [19], which starts with assuming a finite time interval $\mathbb{T} = [0,\ t_{\max})$, where $t_{\max} < +\infty$. As a result, a conclusion is derived as

– *Conclusion* for any compact set $\mathbb{D} \subset \mathbb{I}^3$, there must be a finite time instant $t_{\mathrm{esc}} < t_{\max}$, after which the solution $(e_{\gamma,\mathrm{nor}},\ e_{\alpha,\mathrm{nor}},\ e_{Q,\mathrm{nor}})$ escapes to the outside of $\mathbb{D}$, i.e., $(e_{\gamma,\mathrm{nor}},\ e_{\alpha,\mathrm{nor}},\ e_{Q,\mathrm{nor}}) \in \mathbb{I}^3 - \mathbb{D}$.

However, it is obviously known from (45), (53) and (60) that under the proposed control and the initial condition $(e_{\gamma,\mathrm{nor}}(0),\ e_{\alpha,\mathrm{nor}}(0),\ e_{Q,\mathrm{nor}}(0)) \in \mathbb{I}^3$, the relationship $(e_{\gamma,\mathrm{nor}},\ e_{\alpha,\mathrm{nor}},\ e_{Q,\mathrm{nor}}) \in \cup_{x=\gamma,\alpha,Q}\left[-\frac{2\arctan(\lambda_x)}{\pi}, \frac{2\arctan(\lambda_x)}{\pi}\right] \subset \mathbb{I}^3$ always holds. This relationship indicates that the solution $(e_{\gamma,\mathrm{nor}},\ e_{\alpha,\mathrm{nor}},\ e_{Q,\mathrm{nor}})$ has been strictly constrained within a compact subset of $\mathbb{I}^3$ and cannot escape from the compact set $\cup_{x=\gamma,\alpha,Q}\left[-\frac{2\arctan(\lambda_x)}{\pi}, \frac{2\arctan(\lambda_x)}{\pi}\right]$ during the entire time interval $\mathbb{T}$. The above fact is contradictory with the *Conclusion* derived from the assumption of the finite $\mathbb{T}$, and therefore, the derived stability and performance of the altitude loop can be extended to the infinite $\mathbb{T} = [0,\ +\infty)$.

So far, the design and analysis of the proposed control for both velocity and altitude loops have been finished, whose overall structure is shown in Fig. 1. Note that the state feedback signals are neglected in Fig. 1 for clarity. Though the proposed control is low complexity in both structure and expression, the price paid for this feature is the potential large expense of control actions. Especially for the thermal protection purpose, the maximum CDA and EDA of AHVs are strictly limited, which may have conflict with the possible large control consumption of the low-complexity control in the altitude loop. In practical applications, this problem can be alleviated or solved in the following two aspects. From the perspective of mission planning, less aggressive altitude and FPA references are preferred to reduce the nominal control requirement. In such situation, relatively small deflections of control surfaces are consumed to maintain the ascending or descending maneuver, and thus, there exist enough canard and elevator deflecting margins for the low-complexity control to realize additional objectives (like the AoA constraint accommodation) as well as to overcome multiple factors (like the modeling uncertainty). From the perspective of control realization, selecting proper control gains and performance functions is also an effective way to alleviate the control consumption [9]. For example, it is seen from (44), (52), (59) that lager control gains k_γ, k_α, k_Q in control algorithms (41), (48), (56) are preferred to improve the tracking performance, but probably generate CDA and EDA control signals that cannot be realized by real control surfaces. Therefore, a careful trade-off between tracking performance and control consumption should be made at design level.

4 Simulation study

This section presents a simulation study to verify the proposed control. Nominal parameter values of the AHV model are selected according to [2,22]. Aerodynamic coefficients are supposed to have up to 20% variations around their nominal values. The information of the atmospheric environment, including free air density, free air temperature and Mach number, is simulated according to [17]. In FER saturation (13), $\Phi_{\mathrm{cooling}} = 0.01$, Φ_{choking} is a function related to AoA,

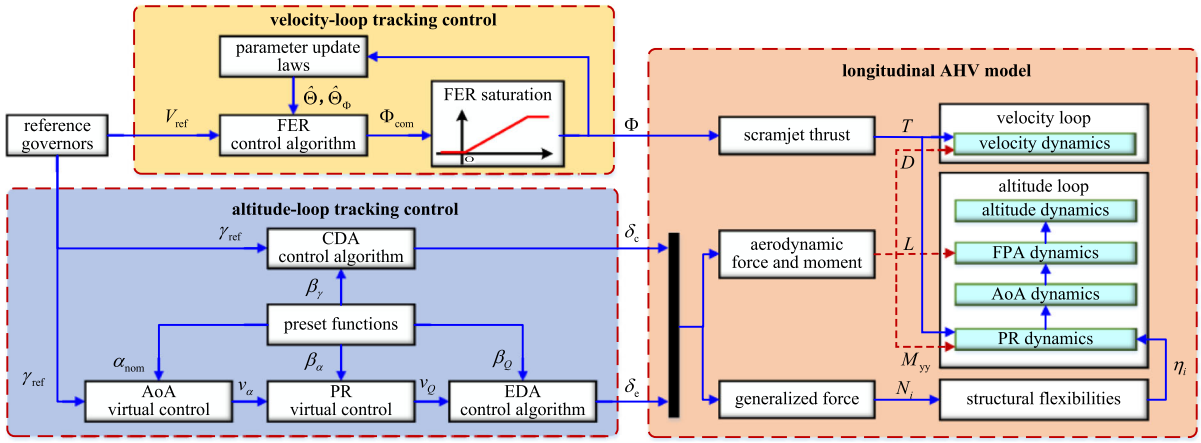

Fig. 1 Overall structure of the proposed control

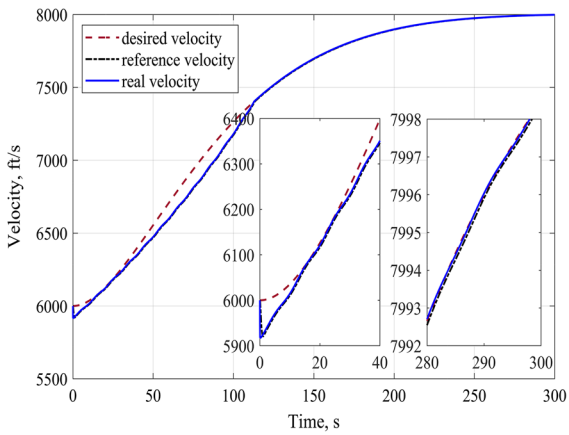

Fig. 2 Velocity tracking result

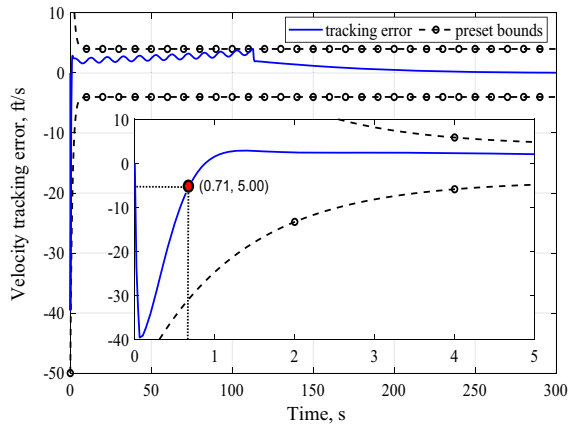

Fig. 3 Velocity tracking error

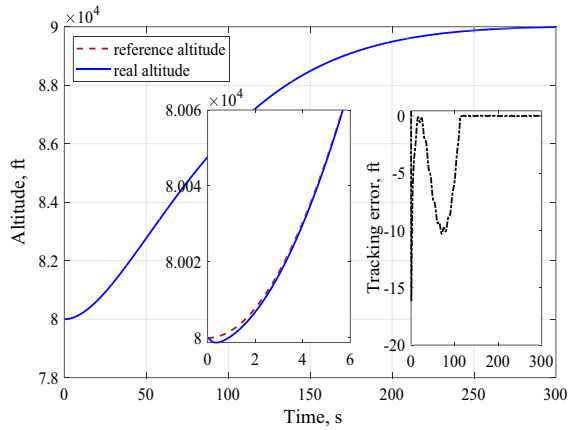

Fig. 4 Altitude tracking result

Mach number and dynamic pressure, whose detailed expression can be found in [38]. In reference governors (14) and (15), $V_{\rm des}$ and $h_{\rm ref}$ are generated using a second-order command filter [16], whose damping ratio and natural frequency are set as 0.9 and 0.02 rad/s, respectively. The initial cruising conditions of the simulated AHV are set as $V = 6000$ ft/s, $h = 80,000$ ft, $\gamma = 0$ deg, $\alpha = 3.5$ deg, $Q = 0$ deg/s, $\eta_1 = 0.832$ ft/slugs$^{1/2}$/ft, $\eta_2 = 0.121$ ft/slugs$^{1/2}$/ft, $\Phi = 0.452$, $\delta_{\rm c} = 2.52$ deg, $\delta_{\rm e} = 15.4$ deg. The simulated AHV implements an accelerating climb with the desired cruising conditions of $V = 8000$ ft/s, $h = 90,000$ ft.

In the velocity loop, suppose the maximal initial velocity tracking error $\varpi_{V,0} = 50$ ft/s, and set the designated tracking precision $\varpi_{V,\rm des} = 5$ ft/s and

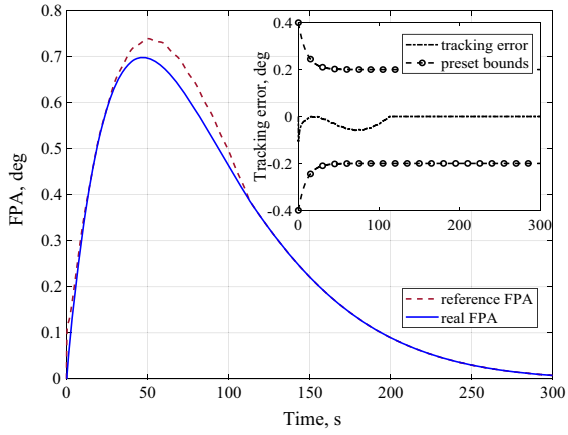

Fig. 5 FPA tracking result

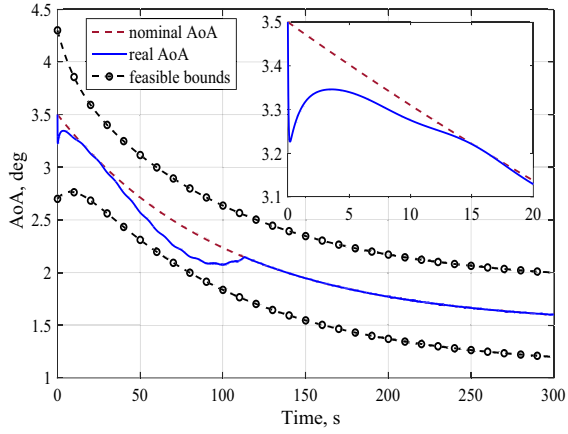

Fig. 6 AoA tracking result

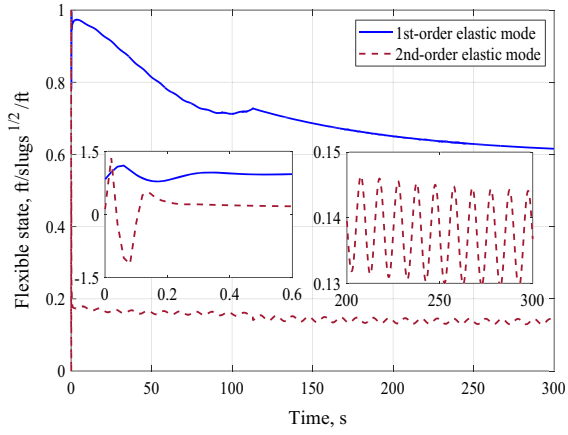

Fig. 7 Generalized elastic coordinates

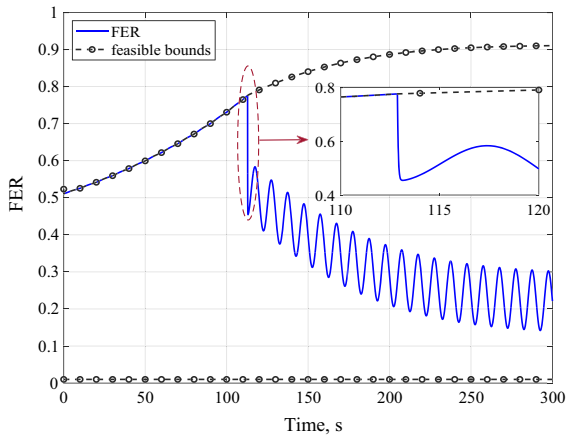

Fig. 8 Control input of FER

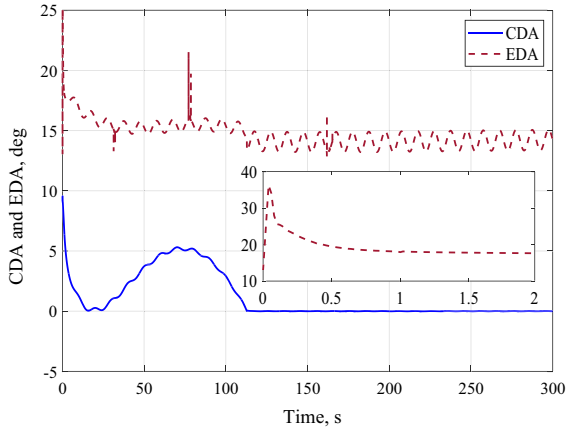

Fig. 9 Control inputs of CDA and EDA

convergence time $t_{V,\mathrm{con}} = 5$ s. Following the rules in Remark 3, parameters in the bound function β_V are selected as $\varpi_{V,\infty} = 5$ and $\tau_V = 0.8$, that is, $\beta_V = 46\mathrm{e}^{-0.8t} + 4$ ft/s. In the altitude loop, set the nominal AoA function $\alpha_{\mathrm{nor}} = 2\mathrm{e}^{-0.01t} + 1.5$ deg and bound functions $\beta_\gamma = \beta_\alpha = 0.2\mathrm{e}^{-0.1t} + 0.2$ deg, $\beta_Q = 10\mathrm{e}^{-0.1t} + 4$ deg/s. As a result, AoA has the asymmetric constraint as $2\mathrm{e}^{-0.01t} - 0.4\mathrm{e}^{-0.1t} + 1.1$ deg $< \alpha(t) < 2\mathrm{e}^{-0.01t} + 0.4\mathrm{e}^{-0.1t} + 1.9$ deg. It should be mentioned that the selection of the bound function β_γ is mainly for the realization of the asymmetric AoA constraint, and the corresponding FPA tracking perfor-

mance index has been properly relaxed to reduce the expense of control actions [9]. For the maximal initial FPA tracking error $\varpi_{\gamma,0} = 0.4$ deg and the tracking precision $\varpi_{\gamma,\mathrm{des}} = 0.25$ deg, the convergence time $t_{\gamma,\mathrm{con}}$ with respect to the selected β_γ can be designated as 15 s. The main control gains are selected as $k_V = 5$, $k_h = 0.02$, $k_\gamma = 0.5$, $k_\alpha = 8$, $k_Q = 25$, and other control gains are properly selected according to the rules in Remark 5. To consider the influence of the atmospheric environment on scramjet, the real thrust output is supposed to have a sinusoidal disturbance whose amplitude is 5% of the nominal thrust output. The corresponding simulation results are given in Figs. 2, 3, 4, 5, 6, 7, 8, 9.

Figures 2 and 3 show tracking results of the velocity loop. It is seen from Fig. 2 that the desired velocity reference cannot be tracked because of the FER saturation property, also see Fig. 8. In this situation, the employed adaptive velocity reference governor generates a modified reference, which is less aggressive and can be well tracked within the ability of scramjet. It is seen from Fig. 3 that the velocity tracking error is regulated between the preset upper and lower bounds, in which case the designated tracking precision and convergence time are guaranteed. In fact, the velocity tracking precision (i.e., $|e_V| < 5$ ft/s) is achieved at $t = 0.71$ s, and the final velocity tracking error becomes smaller than 0.15 ft/s.

Figures 4, 5, 6 show tracking results of the altitude loop. It is seen from Figs. 4 and 5 that the desired altitude reference is well tracked, and the FPA tracking error is regulated between the preset upper and lower bounds. It is seen from Fig. 6 that AoA is regulated around the nominal AoA function without violating the asymmetric constraint. Figure 7 shows the generalized elastic coordinates, indicating that the supposed sinusoidal disturbance on scramjet thrust causes small fluctuations in structural flexibilities.

Figures 8 and 9 show the control input signals of FER, CDA and EDA. It is seen from Fig. 8 that FER becomes saturated soon after the beginning of simulation. After $t = 113$ s, the FER saturation ends when the desired velocity reference becomes less aggressive. Note that FER has some fluctuations to counteract the supposed sinusoidal disturbance on scramjet thrust, and thus, the velocity reference is well tracked. It is seen from Fig. 9 that EDA has slightly fluctuations, which are also affected by the sinusoidal disturbance on the scramjet thrust.

5 Conclusion

A novel longitudinal flight control has been proposed for AHVs, whose main features are the low-complexity algorithm and the handling of the asymmetric AoA constraint. Output tracking errors have been regulated with the designated tracking precision and convergence time, while practical factors including uncertain aerodynamic coefficients, structural flexibilities and FER saturation property have also been taken into account. Both theoretical analysis and simulation results have shown the effectiveness of the proposed control.

Acknowledgements The authors would like to thank the editors and reviewers of Nonlinear Dynamics for their valuable efforts on the review of this paper.

Funding This paper was funded in part by the National Natural Science Foundation of China (Grant No. 61903101), in part by the National Postdoctoral Program for Innovative Talents (Grant No. BX201700064), and in part by the Fundamental Research Funds for the Central Universities (Grant No. HIT.NSRIF.2020021).

Compliance with ethical standards

Conflict of interest The authors declare that they have no conflict of interest.

References

1. An, H., Fidan, B., Liu, J., Wang, C., Wu, L.: Adaptive fault-tolerant control of air-breathing hypersonic vehicles robust to input nonlinearities. Int. J. Control **92**(5), 1044–1060 (2019). https://doi.org/10.1080/00207179.2017.1381346
2. An, H., Liu, J., Wang, C., Wu, L.: Approximate backstepping fault-tolerant control of the flexible air-breathing hypersonic vehicle. IEEE/ASME Trans. Mechatron. **21**(3), 1680–1691 (2016). https://doi.org/10.1109/TMECH.2015.2507186
3. An, H., Liu, J., Wang, C., Wu, L.: Disturbance observer-based antiwindup control for air-breathing hypersonic vehicles. IEEE Trans. Ind. Electron. **63**(5), 3038–3049 (2016). https://doi.org/10.1109/TIE.2016.2516498
4. An, H., Wu, Q., Wang, C., Cao, X.: Simplified fault-tolerant adaptive control of airbreathing hypersonic vehicles. Int. J. Control (2018). https://doi.org/10.1080/00207179.2018.1538569
5. An, H., Wu, Q., Xia, H., Wang, C.: Multiple Lyapunov function-based longitudinal maneuver control of air-breathing hypersonic vehicles. Int. J. Control (2019). https://doi.org/10.1080/00207179.2019.1590650
6. An, H., Xia, H., Wang, C.: Barrier Lyapunov function-based adaptive control for hypersonic flight vehicles. Non-

linear Dyn. **88**(3), 1833–1853 (2017). https://doi.org/10.1007/s11071-017-3347-y
7. Basin, M., Yu, P., Shtessel, Y.: Hypersonic missile adaptive sliding mode control using finite- and fixed-time observers. IEEE Trans. Ind. Electron. **65**(1), 930–941 (2018). https://doi.org/10.1109/TIE.2017.2701776
8. Baumann, E., Pahle, J., Davis, M., White, J.: X-43A flush airdata sensing system flight-test results. J. Spacecr. Rockets **47**(1), 48–61 (2010). https://doi.org/10.2514/1.41163
9. Bechlioulis, C., Rovithakis, G.: A low-complexity global approximation-free control scheme with prescribed performance for unknown pure feedback systems. Automatica **50**(4), 1217–1226 (2014). https://doi.org/10.1016/j.automatica.2014.02.020
10. Bolender, M.: An overview on dynamics and controls modelling of hypersonic vehicles. In: American Control Conference, 2009. ACC'09, pp. 2507–2512. IEEE (2009). https://doi.org/10.1109/ACC.2009.5159864
11. Bolender, M., Doman, D.: Nonlinear longitudinal dynamical model of an air-breathing hypersonic vehicle. J. Spacecr. Rockets **44**(2), 374–387 (2007). https://doi.org/10.2514/1.23370
12. Bu, X.: Envelope-constraint-based tracking control of air-breathing hypersonic vehicles. Aerosp. Sci. Technol. **95**, 105,429 (2019). https://doi.org/10.1016/j.ast.2019.105429
13. Bu, X., Lei, H.: A fuzzy wavelet neural network-based approach to hypersonic flight vehicle direct nonaffine hybrid control. Nonlinear Dyn. **94**(3), 1657–1668 (2018). https://doi.org/10.1007/s11071-018-4447-z
14. Bu, X., Xiao, Y., Lei, H.: An adaptive critic design-based fuzzy neural controller for hypersonic vehicles: predefined behavioral nonaffine control. IEEE/ASME Trans. Mechatron. **24**(4), 1871–1881 (2019). https://doi.org/10.1109/TMECH.2019.2928699
15. Fiorentini, L., Serrani, A.: Adaptive restricted trajectory tracking for a non-minimum phase hypersonic vehicle model. Automatica **48**, 1248–1261 (2012). https://doi.org/10.1016/j.automatica.2012.04.006
16. Fiorentini, L., Serrani, A., Bolender, M., Doman, D.: Nonlinear robust adaptive control of flexible air-breathing hypersonic vehicles. J. Guid. Control Dyn. **32**(2), 402–417 (2009). https://doi.org/10.2514/1.39210
17. Hirschel, E., Weiland, C.: Selected Aerothermodynamic Design Problems of Hypersonic Flight Vehicles. Springer, Berlin (2009)
18. Hu, Q., Wang, C., Li, Y., Huang, J.: Adaptive control for hypersonic vehicles with time-varying faults. IEEE Trans. Aerosp. Electron. Syst. **54**(3), 1442–1455 (2018). https://doi.org/10.1109/TAES.2018.2793319
19. Khalil, H.: Nonlinear Systems, 3rd edn. Prentice Hall, Upper Saddle River (2002)
20. Krstic, M., Kanellakopoulos, I., Kokotovic, P.: Nonlinear and Adaptive Control Design. Wiley, Hoboken (1995)
21. Mu, C., Sun, C., Xu, W.: Fast sliding mode control on air-breathing hypersonic vehicles with transient response analysis. Proc. Inst. Mech. Eng. Part I J. Syst. Control Eng. **230**(1), 23–34 (2016). https://doi.org/10.1177/0959651815609518
22. Parker, J., Serrani, A., Yurkovich, S., Bolender, M., Doman, D.: Control-oriented modeling of an air-breathing hypersonic vehicle. J. Guid. Control Dyn. **30**(3), 856–869 (2007). https://doi.org/10.2514/1.27830
23. Peebles, C.: Road to Mach 10: Lessons Learned from the X-43A Flight Research Program. AIAA, Reston (2008)
24. Serrani, A., Bolender, M.: Addressing limits of operability of the scramjet engine in adaptive control of a generic hypersonic vehicle. In: IEEE 55th Conference on Decision and Control, pp. 7567–7572. IEEE (2016)
25. Shen, Q., Jiang, B., Cocquempot, V.: Fault-tolerant control for TS fuzzy systems with application to near-space hypersonic vehicle with actuator faults. IEEE Trans. Fuzzy Syst. **20**(4), 652–665 (2012). https://doi.org/10.1109/TFUZZ.2011.2181181
26. Shin, J.: Adaptive dynamic surface control for a hypersonic aircraft using neural networks. IEEE Trans. Aerosp. Electron. Syst. **53**(5), 2277–2289 (2017). https://doi.org/10.1109/TAES.2017.2691198
27. Stephen, E., Hoenisch, S., Riggs, C., Waddel, M., McLaughlin, T., Bolender, M.: HIFiRE 6 unstart conditions at off-design mach numbers. In: 53rd AIAA Aerospace Sciences Meeting, pp. 1–19. AIAA (2015)
28. Sun, J., Song, S., Wu, G.: Fault-tolerant track control of hypersonic vehicle based on fast terminal sliding mode. J. Spacecr. Rockets **54**(6), 1304–1316 (2017). https://doi.org/10.2514/1.A33890
29. Wang, N., Wu, H., Guo, L.: Coupling-observer-based nonlinear control for flexible air-breathing hypersonic vehicles. Nonlinear Dyn. **78**(3), 2141–2159 (2014). https://doi.org/10.1007/s11071-014-1572-1
30. Wang, Q., Stengel, R.: Robust nonlinear control of a hypersonic aircraft. J. Guid. Control Dyn. **23**(4), 577–585 (2000). https://doi.org/10.2514/6.1999-4000
31. Wang, Z., Yuan, J.: Full state constrained adaptive fuzzy control for stochastic nonlinear switched systems with input quantization. IEEE Trans. Fuzzy Syst. (2019). https://doi.org/10.1109/TFUZZ.2019.2912150
32. Wang, Z., Yuan, Y., Yang, H.: Adaptive fuzzy tracking control for strict-feedback markov jumping nonlinear systems with actuator failures and unmodeled dynamics. IEEE Trans. Cybern. **50**(1), 126–139 (2020). https://doi.org/10.1109/TCYB.2018.2865677
33. Wang, Z., Zhang, B., Yuan, J.: Decentralized adaptive fault tolerant control for a class of interconnected systems with nonlinear multisource disturbances. J. Frankl. Inst. **355**(11), 4493–4514 (2018). https://doi.org/10.1016/j.jfranklin.2017.10.038
34. Xu, B., Shi, Z.: An overview on flight dynamics and control approaches for hypersonic vehicles. Sci. China Inf. Sci. **58**(7), 1–19 (2015). https://doi.org/10.1007/s11432-014-5273-7
35. Xu, B., Shi, Z., Sun, F., He, W.: Barrier Lyapunov function based learning control of hypersonic flight vehicle with AOA constraint and actuator faults. IEEE Trans. Cybern. **49**(3), 1147–1157 (2018). https://doi.org/10.1109/TCYB.2018.2794972
36. Xu, B., Wang, D., Zhang, Y., Shi, Z.: DOB based neural control of flexible hypersonic flight vehicle considering wind effects. IEEE Trans. Ind. Electron. **64**(11), 8676–8685 (2017). https://doi.org/10.1109/TIE.2017.2703678
37. Xu, H., Mirmirani, M., Ioannou, P.: Adaptive sliding mode control design for a hypersonic flight vehicle. J. Guid. Control Dyn. **27**(5), 829–838 (2004). https://doi.org/10.2514/1.12596

38. Zinnecker, A., Serrani, A., Bolender, M., Doman, D.: Combined reference governor and anti-windup design for constrained hypersonic vehicles models. In: AIAA Guidance, Navigation, and Control Conference, pp. 1–20. AIAA 2009–6283 (2009)